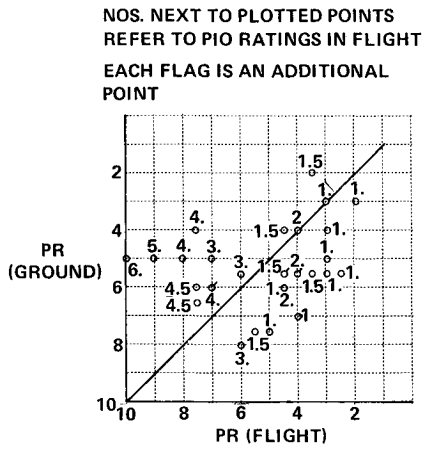

Fig. 10 Comparison of pilot ratings in flight and in a fixed base ground simulator—pilot H.

A comparison of fixed-base ground simulator vs flight evaluations indicates that configurations with significant PIO tendencies are rated poorer in flight than on the ground. In evaluating PIO tendencies, ground simulator results are not conservative and can be very misleading.

References

[1] Parrag, M. L., "Pilot Evaluation in a Ground Simulator of the Effects of Elevator Control System Dynamics in Fighter Aircraft," AFFDL-TR-67-19, Sept. 1967, Cornell Aeronautical Lab., Buffalo, N. Y.

[2] Key, D. L., "A Functional Description and Working Data for the Variable Stability System T-33 Airplane," Rept. TC-1921-F-2, Oct. 1965, Cornell Aeronautical Lab., Buffalo, N. Y.

[3] Chalk, C. R., "Simulator Investigation of the Effects of L_α and True Speed on Longitudinal Handling Qualities," *Journal of Aircraft*, Vol. 1, No. 6, Nov.–Dec. 1964, pp. 335–344.

[4] Bihrle, W., Jr., "A Handling Qualities Theory for Precise Flight Path Control," AFFDL-TR-65-198, June 1966, Wantagh, N. Y.

[5] DiFranco, D. A., "Flight Investigation of Longitudinal Short Period Frequency Requirements and PIO Tendencies," AFFDL-TR-66-163, April 1967, Cornell Aeronautical Lab., Buffalo, N. Y.

[6] DiFranco, D. A., "In-Flight Investigation of the Effects of Higher-Order Control System Dynamics on Longitudinal Handling Qualities," AFFDL-TR-68-90, July 1968, Cornell Aeronautical Lab., Buffalo, N. Y.

[7] Harper, R. P., Jr. and Cooper, G. E., "A Revised Pilot Rating Scale for the Evaluation of Handling Qualities," AGARD C.P. 17, Sept. 20–23, 1966, Compilation of papers presented to AGARD Flight Mechanics Panel Specialists' Meeting, Cambridge, England.

SEPT.-OCT. 1970 J. AIRCRAFT VOL. 7, NO. 9

Altitude Stability in Supersonic Cruising Flight

ROBERT F. STENGEL*
Massachusetts Institute of Technology, Cambridge, Mass.

The importance of maintaining a fixed altitude is increased for aircraft cruising at supersonic speed. The difficulties of altitude control are enhanced by the small flight-path angle required to cause large vertical rates and by the time scale and basic instability of the long-period motion. The causes of altitude deviation, the magnitude of their effects, and the stability of the motion are defined for a wide range of altitudes and Mach numbers and for aircraft of varying lift-drag ratio, wing loading, thrust law, and pitch dynamics. In addition to suggesting necessary and favorable control laws, the effects of horizontal and vertical wind, atmospheric state variation, and engine "unstarts" are treated.

Nomenclature

A = coefficient matrix of the homogeneous equation
a = sound speed, fps
a_i = characteristic equation coefficient
AR = wing aspect ratio
B = scaling matrix for control inputs
C = scaling matrix for disturbance inputs
c = mean aerodynamic chord, ft
C_D = drag coefficient (additional subscript denotes a partial derivative)
C_L = lift coefficient (additional subscript denotes a partial derivative)
C_m = moment coefficient (additional subscript denotes a partial derivative)
DT_u = $g[2 - \nu' - M^2/(M^2 - 1)]/U(L/D)$
D_α = $2gC_{L\alpha}/\pi eAR$
D_δ = $gC_{D\delta}/C_L$
D_ξ = drag scaling coefficient for general disturbance
e = efficiency factor for drag-due-to-lift
G = compensation transfer function
g = acceleration-due-to-gravity, fps^2
j = $(-1)^{1/2}$
k = radius of gyration, ft
L/D = lift-drag ratio
L_h = $g[a_h/a(1 - 1/M^2) - \beta]$
L_p = g/p
L_u = $g[2 - M^2/(M^2 - 1)]/U$
L_α = $gC_{L\alpha}/C_L$
L_δ = $gC_{L\delta}/C_L$
L_ξ = lift scaling coefficient for general disturbance
L_ρ = g/ρ
M = Mach number
m = mass, slugs
M_h = $T_h r/k^2$ (aerodynamic and aeroelastic contributions not included explicitly)
M_p = $gr/pk^2(L/D)$
M_{Th} = $gr/k^2(L/D)$

Received July 7, 1969; presented as Paper 69-813 at the AIAA Aircraft Design and Operations Meeting, July 14–16, 1969, Los Angeles, Calif.; revision received January 7, 1970.

* Member of the Research Staff, Charles Stark Draper Laboratory. Member AIAA.

M_u = $T_u r/k^2$ (aerodynamic and aeroelastic contributions not included explicitly)
M_α = $g\bar{x}C_{L_\alpha}/k^2C_L$
$M_{\dot\alpha}$ = $-\pi gc^2/18k^2UC_L$ (from Ref. 14, assuming triangular wing)
M_δ = gcC_{m_δ}/k^2C_L
$M_{\dot\theta}$ = $3M_{\dot\alpha}$ (from Ref. 14, assuming triangular wing)
M_ξ = moment scaling coefficient for general disturbance
M_ρ = $gr/\rho k^2(L/D)$
N_ξ^h = open-loop altitude transfer function numerator for general disturbance
$N_{\xi^h\delta^\eta}$ = coupling numerator for altitude response to general disturbance with single loop closure
r = thrust axis offset, ft
S = wing area, ft^2
s = laplace operator
T_p = phugoid time constant, sec
T_{Th} = $g/(L/D)$
U = forward velocity, fps
W = weight, lb
$\mathbf{x}$ = dependent variable vector
$\bar{x}$ = aerodynamic center position, ft (negative aft of center-of-gravity)
β = air density inverse scale height, ft^{-1}
Δ = characteristic equation
Δh = altitude perturbation variable, ft
Δp = pressure disturbance, millibars
ΔT = temperature disturbance, °F
ΔTh = thrust disturbance, %
Δu = forward velocity perturbation variable, fps
Δu_w = horizontal wind disturbance, fps
Δw_w = vertical wind disturbance, fps
$\Delta\alpha$ = angle-of-attack perturbation variable, deg
$\Delta\gamma$ = flight path angle perturbation variable, deg
$\Delta\delta$ = control deflection
$\Delta\eta$ = general perturbation variable
$\Delta\theta$ = pitch attitude angle perturbation variable, deg
$\Delta\xi$ = general disturbance
$\Delta\rho$ = air density disturbance, slug-ft^{-3}
δ = control deflection vector
ϵ = disturbance vector
ζ_p; ζ_{sp} = phugoid damping ratio; short period damping ratio, respectively
λ_h = height mode pole, sec^{-1}
ν = exponent of thrust velocity dependence
ν' = ν(1 − static thrust/full thrust)
ρ = air density, slugs-ft^{-3}
τ_h = height mode time constant, sec
ϕ = transfer function phase angle, deg
ω_p; ω_{sp} = phugoid frequency; short period frequency respectively, rad/sec

I. Introduction

AMONG the dynamical problems of supersonic cruising flight, altitude stability has, until recently, drawn the least attention. The lack of concern has been warranted, since the short period modes are most closely associated with attitudes, acceleration, and flight-path control, which have required extensive study. Furthermore, all supersonically cruising aircraft have been experimental or military aircraft, which presumably have air space priority unmatched by civil aircraft. The advent of the supersonic transport brings new weight to the study of altitude stability, for such an aircraft must fly within a densely populated system of air lanes and must operate economically.

There is cause for concern in reports of flight and simulator tests. At a meeting of the Society of Experimental Test Pilots, pilots of this nation's supersonically cruising aircraft commented on the long period of the phugoid mode, indicating that wide altitude spacing of supersonic traffic might be a consequence of the oscillation.[1] Alvin S. White estimated "that a 10,000-ft altitude separation would have been required with instruments used in the XB-70."[1] In one simulator study of a supersonic transport, pilots deviated from the preassigned altitude by at least 500 ft in 80% of the runs.[2] Another report[3] indicates that upset recovery is prolonged at high speeds and 16,000–17,000-ft altitude may be required for the recovery. Several speakers at a technical symposium on the supersonic transport[4] confirmed that high pitch angle resolution of aircraft instruments is critical for altitude hold. Speaking at that meeting, White suggested that pressure gradients are significant and that improved altimetry (possibly inertial) is needed.

Newell and Campbell report good correlation between phugoid damping and the power spectral density of altitude variation.[5] Areas under the spectral curves indicate altitude standard deviations of 500–1400 ft for damping ratios of 0.28–−0.15 and for 200-mph air speed. The pilot could concentrate on the poorly damped phugoid for no longer than 5 min; then, other flying duties demanded his attention.

Altitude stability first received attention from Lanchester, who defined phugoid motion in 1897 as the oscillating interchange of potential and kinetic energy.[6] Lanchester's nonlinear solution neglected atmospheric damping and rotational dynamics, which were added in later linearized treatments. In 1942, Schuebel recognized the importance of the air density gradient in limiting the phugoid period.[7] Neumark added the effects of thrust and of sound speed variation with altitude.[8] In his hallmark paper of 1950, he defined the characteristic equation of longitudinal motion as quintic rather than quartic. This paper also considered the stability of supersonic flight. Etkin pursued this development into orbit, adding spherical earth effects.[9] He found that the thrust law has significant effect on phugoid damping. Larrabee considers a thrust law proportional to a power of air speed other than two in a 1967 paper.[10]

II. Dynamical Equations

The linearized equations-of-motion for longitudinal flight are derived in several texts; those presented follow Seckel.[11] The linearized equations provide solutions for perturbations from an initial flight condition, and all equation coefficients are computed on the basis of the nominal altitude and speed. The coefficients of the equations are dimensional stability derivatives, relating acceleration sensitivities to perturbations in "real time."

Typically, there are three equations in the longitudinal set, and these are based on the perturbation variables Δu (forward velocity), $\Delta\alpha$ (angle-of-attack) or Δw (normal velocity), and $\Delta\theta$ (pitch attitude angle). Since altitude-dependent effects will be considered, it is necessary to append the kinematic relation between the altitude perturbation (Δh) and the flight-path perturbation angle ($\Delta\gamma$): $d(\Delta h)/dt = U\Delta\gamma$ and $\Delta\gamma = \Delta\theta - \Delta\alpha$.

Transforming the ordinary differential equations-of-motion by the Laplace transform and neglecting initial conditions,

$$\mathbf{A}(s)\mathbf{x}(s) = \mathbf{B}\delta(s) + \mathbf{C}(s)\boldsymbol{\epsilon}(s) \tag{1}$$

where the terms of Eq. (1) are defined by Eqs. (2–7):

$$\mathbf{A}(s) = \begin{bmatrix} (s + DT_u) & (D_\alpha - g) & g & 0 \\ L_u/U & (s + L_\alpha/U) & -s & L_h/U \\ -M_u & -(M_{\dot\alpha}s + M_\alpha) & s(s - M_{\dot\theta}) & -M_h \\ 0 & U & -U & s \end{bmatrix} \tag{2}$$

$$\mathbf{x}^T(s) = [\Delta u(s)\,\Delta\alpha(s)\,\Delta\theta(s)\,\Delta h(s)] \tag{3}$$

$$\mathbf{B} = \begin{bmatrix} -D_{\delta T} & -D_{\delta L} & -D_{\delta M} & 0 \\ -L_{\delta T}/U & -L_{\delta L}/U & -L_{\delta M}/U & 0 \\ M_{\delta T} & M_{\delta L} & M_{\delta M} & 0 \\ 0 & 0 & 0 & 0 \end{bmatrix} \tag{4}$$

$$\boldsymbol{\delta}^T(s) = [\Delta\delta_t(s)\,\Delta\delta_L(s)\,\Delta\delta_M(s)0] \tag{5}$$

$$\mathbf{C}(s) = \begin{bmatrix} -DT_u & -D_\alpha/U & 0 \\ -L_{u_w}/U & -L_\alpha/U^2 & -L_\rho/U \\ M_{u_w} & [(M_{\dot\alpha} - M_{\dot\theta})s + M_\alpha]/U & M_\rho \\ 0 & 0 & 0 \end{bmatrix} \begin{bmatrix} 0 & 0 & T_{Th} \\ -L_T/U & -L_p/U & 0 \\ 0 & M_p & M_{Th} \\ 0 & 0 & 0 \end{bmatrix} \quad (6)$$

$$\epsilon^T(s) = [\Delta u_w(s)\, \Delta w_w(s)\, \Delta\rho(s)\, \Delta T(s)\, \Delta p(s)\, \Delta Th(s)] \quad (7)$$

It is not necessary to eliminate a variable before proceeding; however, a 3×3 matrix is easier to visualize and expand than a 4×4 matrix. Using the relationship between altitude, and angle-of-attack, $\Delta\theta$ and $\Delta\alpha$ are consecutively eliminated in Eqs. (8) and (9).

$$\mathbf{A}_1(s)\mathbf{x}(s) = \begin{bmatrix} (s + DT_u) & D_\alpha & gs/U \\ L_u/U & L_\alpha/U & -(s^2 - L_h)/U \\ -M_u & [s^2 - (M_{\dot\alpha} + M_{\dot\theta})s - M_\alpha] & (s^3/U - M_{\dot\theta}s^2/U - M_h) \end{bmatrix} \begin{bmatrix} \Delta u \\ \Delta\alpha \\ \Delta h \end{bmatrix} \quad (8)$$

$$\mathbf{A}_2(s)\mathbf{x}(s) = \begin{bmatrix} (s + DT_u) & D_\alpha & -(D_\alpha - g)s/U \\ L_u/U & L_\alpha/U & -(s^2 + L_\alpha s/U - L_h)/U \\ -M_u & [s^2 - (M_{\dot\alpha} + M_{\dot\theta})s - M_\alpha] & (M_{\dot\alpha}s^2/U + M_\alpha/U - M_h) \end{bmatrix} \begin{bmatrix} \Delta u \\ \Delta\theta \\ \Delta h \end{bmatrix} \quad (9)$$

The determinants of $\mathbf{A}_1(s)$ and $\mathbf{A}_2(s)$ are equal, yielding a characteristic equation of the form shown in Eq. (10):

$$\Delta = (a_6\lambda^5 + a_5\lambda^4 + a_4\lambda^3 + a_3\lambda^2 + a_2\lambda + a_1)/U = 0 \quad (10)$$

Typically, Eq. (10) can be factored to Eq. (11) as follows:

$$(\lambda - \lambda_h)(\lambda^2 + 2\zeta_p\omega_p\lambda + \omega_p^2) \times (\lambda^2 + 2\zeta_{sp}\omega_{sp}\lambda + \omega_{sp}^2)/U = 0 \quad (11)$$

Longitudinal Modes and Their Approximations

The roots of these equations are precisely determined only by iterative techniques; however, if the singularities are widely spaced, as is generally the case in supersonic flight, good approximations can be found without factoring Eq. (10).

With prior knowledge of the characteristic equation's roots, we can identify the height mode, the phugoid mode, and the short period mode. It is reasonable to associate these modes with ascending powers of λ, which relate to the higher derivatives of the dependent variables and, thus, to higher frequency motion.

Inspection of Eq. (10) and a multitude of numerical examples indicate that the height mode pole $\lambda_{h3\text{dof}}$ can be approximated by a_1/a_2. The height mode owes its existence to the forces and moments that vary with height; without them, a_1 would vanish, and a "free λ" could be factored from Eq. (10).

Similarly, neglecting the $\Delta\alpha$ degree-of-freedom,

$$\lambda_{h2\text{dof}} \approx DT_uL_h/(L_h - gL_u/U) \quad (12)$$

Using the next three coefficients of the quintic equation to describe the phugoid mode, it is found that the natural frequency is approximated by $(a_2/a_4)^{1/2}$, while the damping ratio is approximately $a_3/2(a_2a_4)^{1/2}$.

The corresponding two d-o-f approximations are

$$\omega_{p2\text{dof}} \approx (L_ug/U - L_h)^{1/2} \quad (13)$$

and

$$\zeta_{p2\text{dof}} \approx DT_u/2(L_ug/U - L_h)^{1/2} \quad (14)$$

The stability derivatives are based upon common simplifications. For example, lift slope is proportional to $(M^2 - 1)^{-1/2}$, air density varies exponentially with the inverse scale height (β), and sound speed is a linear function $(a_hh + a_0)$ of altitude. Substituting for the stability derivatives,

$$\omega_{p2\text{dof}} \approx \{g[2_g/U^2 + \beta - (M^2/(M^2 - 1)) \times (a_h/a + g/U^2)]\}^{1/2} \quad (15)$$

The limiting effect of increasing speed can be seen, for (neglecting spherical earth terms),

$$\omega_{p2\text{dof}} \xrightarrow[U,\, M\to\infty]{} [g(\beta - a_h/a)]^{1/2} \quad (16)$$

Similarly, with thrust slope (ν'), the damping ratio is

$$\zeta_{p2\text{dof}} \approx g[2 - \nu' - M^2/(M^2 - 1)]/2U(L/D)\omega_{p2\text{dof}} \quad (17)$$

As L/D increases, the numerical value of $\zeta_{p2\text{dof}}$ decreases. If thrust grows faster than drag with increasing velocity, $\zeta_{p2\text{dof}}$ is negative.

In the parametric study of phugoid and height mode roots that follows, the short period will be handled in two ways. First, the static margin is chosen to yield a natural frequency of 1.5 rad/sec in the "standard case," and M_α and $M_{\dot\theta}$ are allowed to change with parameter variations. In the second approach, M_α and $M_{\dot\theta}$ are augmented to simulate a stabilization system; the resulting pole and zero locations are identical to those that would be obtained with angle-of-attack and pitch-rate feedback. The short period frequency and damping ratio are maintained close to 2.5 rad/sec and 0.45 for acceptable handling qualities.

Relationship between Altitude and Pitch Angle

In the absence of forcing functions, the relationship between altitude (Δh) and pitch angle perturbations $(\Delta\theta)$ can be obtained from the coefficient matrix of Eq. (9). It is,

$$\frac{\Delta h(s)}{\Delta\theta(s)} = \frac{s^2 - (M_{\dot\alpha} + M_{\dot\theta})s + (M_uL_\alpha/L_u - M_\alpha)}{(M_u/L_u - M_{\dot\alpha}/U)s^2 + (M_uL_\alpha/UL_u - M_\alpha/U)s + (M_h - M_uL_h/L_u)} \quad (18)$$

The Lanchester approximation required that $\Delta h(s)/\Delta\theta(s)|_{2\text{dof}} = U/s$. This is obtained from the zeroth-order numerator and first-order denominator terms of Eq. (18), indicating what must be negligible for the two d-o-f case to be valid.

The frequency response is obtained by substituting $j\omega$ for s in Eq. (18). Unlike the two d-o-f case, low-frequency response may be bounded, and high-frequency response does not go to zero (although the rigid body, steady aerodynamic model breaks down at high frequency). As ω goes to zero, the step response gain is found to be

$$\Delta h(0)/\Delta\theta(0) = (M_\alpha L_u - M_uL_\alpha)/(M_uL_h - L_uM_h) \quad (19)$$

Equation (19) is unbounded if the denominator is zero—the case if height derivatives were neglected. Results, presented in a later section, show that the two d-o-f case is a good approximation in a range of intermediate frequencies, and it is exceptional at the phugoid frequency. The zeros of Eq. (18)

form a complex pair near the short period poles, while the denominator is most often composed of two real roots.

Relationship between Altitude and Angle-of-Attack

Beginning with Eq. (8), the $\Delta h/\Delta\alpha$ transfer function is found to be

$$\frac{\Delta h(s)}{\Delta\alpha(s)} = \frac{-[s^2 - (M_{\dot\alpha} + M_{\dot\theta})s + (M_u L_\alpha/L_u - M_\alpha)]}{s^3/U - (M_{\dot\theta}/U + M_u/L_u)s^2 + (0)s + (M_u L_h/L_u - M_h)} \quad (20)$$

The numerator is the same as the $\Delta h/\Delta\theta$ numerator, and

$$\Delta h(0)/\Delta\alpha(0) = (M_\alpha L_u - M_u L_\alpha)/(M_u L_h - M_h L_u) \quad (21)$$

indicating that $\Delta\alpha$ and $\Delta\theta$ are equal when the final response to an input step is reached.

The two d-o-f case gives no information on $\Delta h/\Delta\alpha$, since $\Delta\alpha$ is identically zero at all frequencies. It might be assumed, however, that where the 2 d-o-f approximation is valid, oscillation in Δh is accompanied by a very small $\Delta\alpha$ oscillation, i.e., that $\Delta h/\Delta\alpha$ is very large.

Transfer Function Numerators

The denominator of all control and disturbance transfer functions is the characteristic equation [Eq. (10)]. The numerator of the transfer function relating a perturbation variable to an input is obtained by replacing the $A(s)$ column, which multiplies the variable with the scaling column of the input, then evaluating the determinant of this new matrix. A single-loop closure modifies the roots of the closed-loop characteristic equation but does not change the zeros of the transfer function. It may alter the zeros of other transfer functions,[12] and poles and zeros of disturbance response transfer functions can be altered by the single-loop closure.

The numerators for altitude response to disturbances all take a single form. Calling $\Delta\xi$ the general disturbance input, the numerator of the $\Delta h/\Delta\xi$ transfer function is

$$N_\xi{}^h = -D_\xi L_u[s^2 - (M_{\dot\alpha} + M_{\dot\theta})s + (M_u L_\alpha/L_u - M_\alpha)]/U + M_\xi L_\alpha[s + (DT_u - D_\alpha L_u/L_\alpha)]/U + L_\xi\{s^3 + [DT_u - (M_{\dot\alpha} + M_{\dot\theta})]s^2 + [-M_\alpha - DT_u(M_{\dot\alpha} + M_{\dot\theta})]s + (D_\alpha M_u - DT_u M_\alpha)\}/U \quad (22)$$

and the transfer function is $\Delta h(s)/\Delta\xi(s) = N_\xi{}^h/\Delta$.

With a single-loop closure of the general perturbation variable $\Delta\eta$ to the control deflection $\Delta\delta$, McRuer, Ashkenas, and Pass[12] show that the disturbance response transfer function becomes

$$\Delta h(s)/\Delta\xi(s)|_{\eta\to\delta} = (N_\xi{}^h + GN_\xi{}^h{}_\delta{}^\eta)/(\Delta + GN_\delta{}^\eta) \quad (23)$$

where G is a feedback compensation, $N_\delta{}^\eta$ is the single-loop closure numerator, and $N_\xi{}^h{}_\delta{}^\eta$ is the coupling numerator. The coupling numerator is found by replacing the Δh and $\Delta\eta$ columns of $\mathbf{A}(s)$ with the scaling columns of $\Delta\xi$ and $\Delta\delta$.

III. Numerical Results

Parametric Sweep

In this section, parametric variations in the height and phugoid mode roots are charted. Cruising altitude, cruising speed (U), wing loading (W/S), lift-to-drag ratio (L/D), thrust law slope (ν'), "speed stability" (M_u), moment due to altitude change (M_h), and short period stability are varied.

Starting from a "standard case," each of the first five parameters is swept individually for two thrust offset and two short period stability conditions. The standard case is representative of a supersonic transport cruising at Mach 3 at 70,000-ft altitude; L/D is 8, W/S is 60 psf, and ν' is +2. Additional characteristics are: k = 32.7 ft, AR = 2, $C_{L\alpha}$ = 1.55 rad^{-1}, e = 0.35, c = 50 ft, S = 5000 ft^2, $C_{D\delta}$ = 0.045 rad^{-1}, $\bar{x}$ = −5 ft, W = 300,000 lb^{-1}, and $C_{m\delta}$ = 0.25 rad^{-1}.

The parameters are varied as follows: altitude: 40,000–115,000 ft, Mach number: 2–6, wing loading: 30–120 psf, lift/drag: 4–12, thrust-axis offset: −24 to +24 ft, and short period stability: augmented or unaugmented.

Altitude is the first parameter to be varied, and the results are shown in Fig. 1. Three cases are illustrated. For the first two, there is no thrust offset (r), and M_u and M_h are assumed to be zero; short period roots are augmented and unaugmented. In the third case, there is a 6-ft thrust offset causing nonzero M_u and M_h, and the short period is augmented.

The phugoid period (T_p) fits the trend of Eq. (15). The value of β derived from the U.S. Standard Atmosphere, 1962,[13] fluctuates with increasing altitude, first decreasing, then increasing, then decreasing again. The inverse of this pattern is discernible in T_p. The period T_p is greater at low altitudes with the augmented short period (r = 0) because of the effect of $M_{\dot\theta}$ in a_2 of Eq. (10), but for 6-ft thrust offset, the leading term of a_2 becomes significant. As altitude increases, L_α decreases, and this effect is diminished. The phugoid period ranges from 149 to 170 sec, with all three cases approaching 159.5 sec at 115,000 ft.

The damping ratio (ζ_p) is negative at all altitudes, and the phugoid mode is unstable. With the augmented short period, the phugoid becomes less unstable with altitude. The increase of $M_{\dot\theta}$ in order to maintain short period stability has a mild stabilizing effect on the phugoid mode. In the altitude sweep, ζ_p ranges from 0.0000355 to −0.0026.

The height mode is unstable, but the divergence is weak; τ_h (the inverse of λ_h) ranges from 700–760 sec.

Mach number effects are plotted in Fig. 2. The unaugmented phugoid period climbs slowly toward its limiting value of 162.1 sec, as given by Eq. (16). The period is increased by the decreasing amount of short period augmentation and is increased by $L_\alpha M_u$ in a_2. The phugoid wavelength (L_p) increases with velocity, ranging from 49 to 162 mi. The phugoid becomes less unstable with increasing M as the

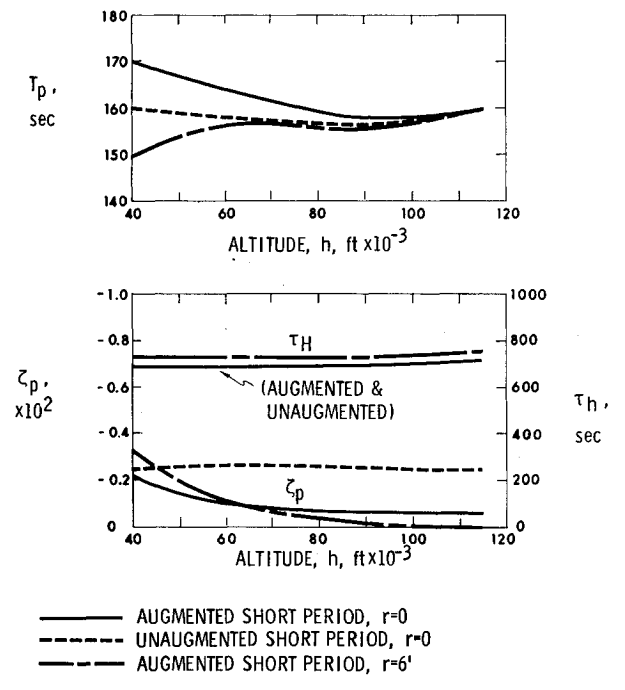

Fig. 1 Cruising altitude effect on th phugoid and height modes.

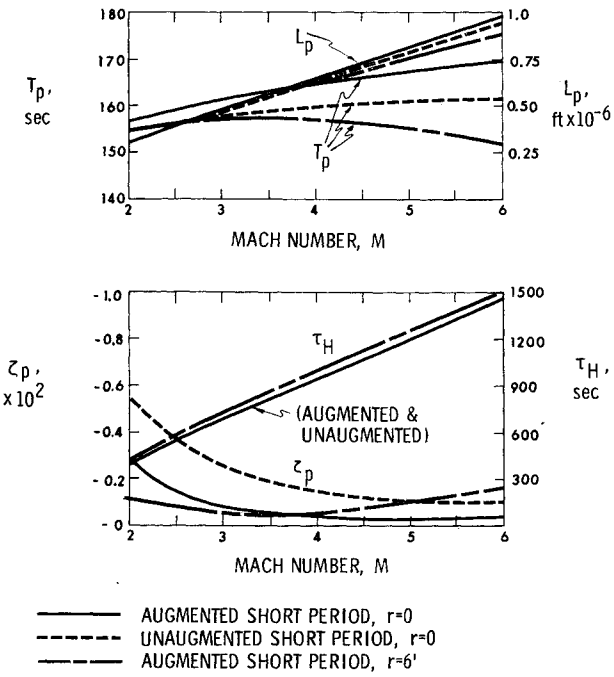

Fig. 2 Cruising Mach number effect on the phugoid and height modes.

magnitude of DT_u diminishes (DT_u is negative and has a destabilizing effect). For the offset thrust case, M_u decreases, and its stabilizing effect is reduced. The height mode time constant increases by a factor of three as DT_u becomes smaller, ranging between 408 and 1488 sec.

The quantity T_p is largely independent of L/D (Fig. 3). As indicated by Eq. (17), low L/D enlarges the magnitude of ζ_p, whether it is positive or negative; in this case, it adds to the instability. A similar effect is seen in τ_h, where low L/D hastens the divergence.

Thrust law slope (ν') has negligible effect on T_p, but it produces large changes in ζ_p and τ_h. The thrust model used

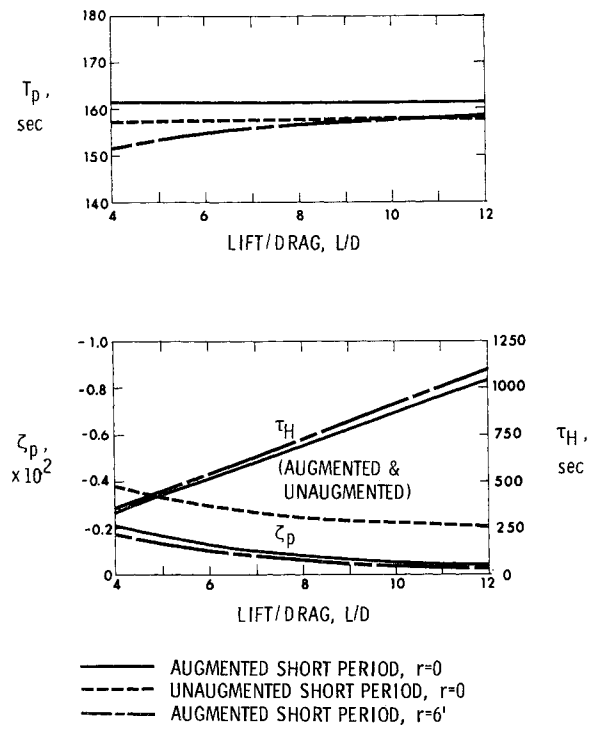

Fig. 3 Lift/drag ratio effect on the phugoid and height modes.

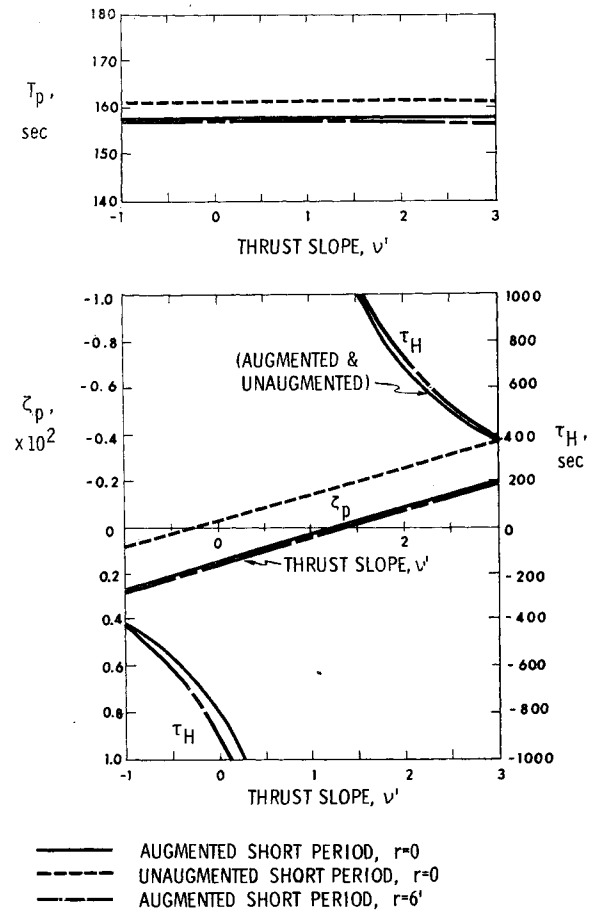

Fig. 4 Thrust slope effect on the phugoid and height modes

in this paper consists of a static term and a term proportional to U^{ν}. As U increases, thrust increases along a local slope of ν', a function of ν and the ratio of static-to-full thrust. Phugoid damping and height mode time constant are strongly dependent on the difference between drag and thrust growth with velocity; i.e., on DT_u, which ν' enters directly. Figure

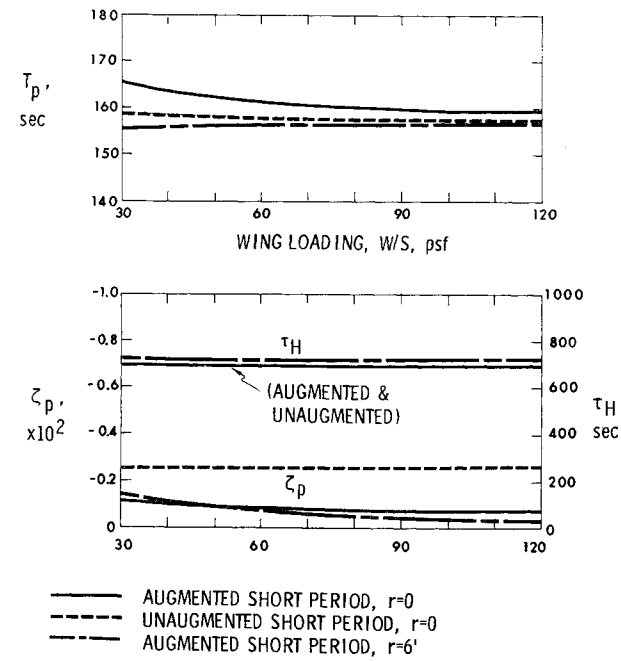

Fig. 5 Wing loading effect on the phugoid and height modes.

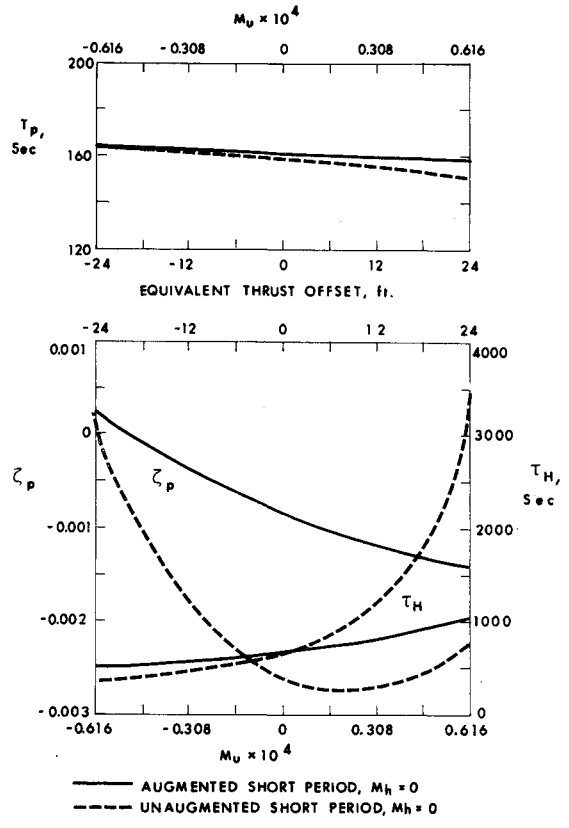

Fig. 6 Speed stability effect on the phugoid and height modes.

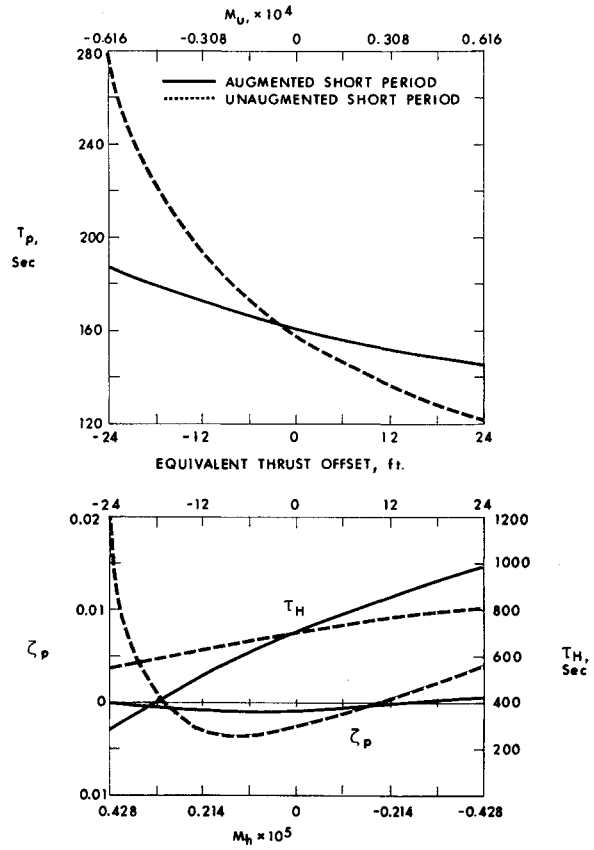

Fig. 7 Thrust offset effect on the phugoid and height modes.

4 illustrates the progression from stability to instability as ν' goes from -1 to $+3$.

Wing loading has a rather small effect on T_p, ζ_p, and τ_h. Figure 5 indicates that the trends with increasing W/S are similar to those of increasing altitude.

The speed stability derivative (M_u) has little effect of the phugoid period but has substantial effect on ζ_p and τ_h. It is assumed that M_u derives from thrust offset entirely, so this parameter is varied through the offset distance r. The offset distance also affects M_h, but M_h is arbitrarily set to zero for Fig. 6. If M_u is positive, there is an increased tendency to nose up at the bottom of the phugoid oscillation, where forward velocity is highest. The opposite occurs at the peak of the motion. Consequently, the period of the motion is decreased. The forward velocity perturbation is in-phase with pitch rate, so negative M_u aids phugoid damping.

Density variation with altitude induces thrust change, which, combined with an offset thrust axis, introduces the stability derivative (M_h) that is added to the M_u variation of Fig. 7. (It is present for all thrust offsets except those of the previous figure.) Altitude and velocity perturbations are out-of-phase at the phugoid frequency, causing M_u and M_h, which have opposite signs, to work together. Comparison of Figs. 6 and 7 shows M_h to be the dominant term, providing phugoid stability at high- and low-thrust offsets and shifting T_p between limits of 144 and 187 sec for the augmented case. As M_h is varied between its positive and negative limits, τ_h travels from 290 to nearly 1000 sec.

The phugoid and height mode roots of a supersonically cruising aircraft always lie near the $j\omega$ axis of the s plane; most often they are in the right half plane. A stability augmentation system which augments only the short period is insufficient to stabilize these motions, although the rates of divergence are slow enough to be perceived by an alert pilot.

The most negative phugoid damping ratio found here is -0.006; combinations of parameters, e.g., low altitude and Mach number, could heighten the instability. Similarly, the most divergent height mode, which has a 280-sec time constant, could become more severe with the added effects of low L/D, high-thrust slope, negative M_u, and positive M_h. Phugoid period remains within 11 sec of 160 sec for all but large values of $|M_h|$.

Transfer Functions

The $\Delta h/\Delta\theta$ transfer functions of Fig. 8 give clear evidence for the two d-o-f approximation. Setting Δh equal to $U\Delta\theta/j\omega$ results in an amplitude ratio with -20 db/decade slope and a phase angle of $-90°$. The standard case, with and without short period augmentation, coincides with the approximation up to a 0.5-rad/sec frequency, where short period dynamics first become significant. Complex zeros near the short period poles decrease $|\Delta h/\Delta\theta|$, indicating that short period oscillations produce little altitude change.

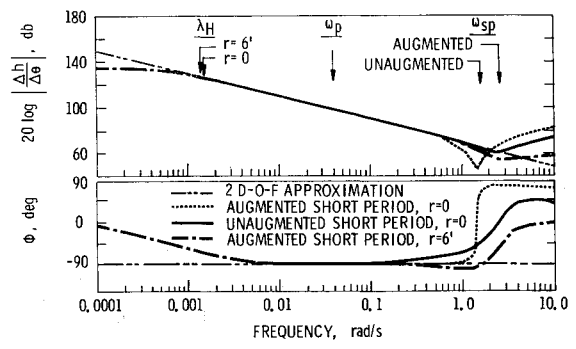

Fig. 8 Altitude/pitch angle frequency response, short period effects.

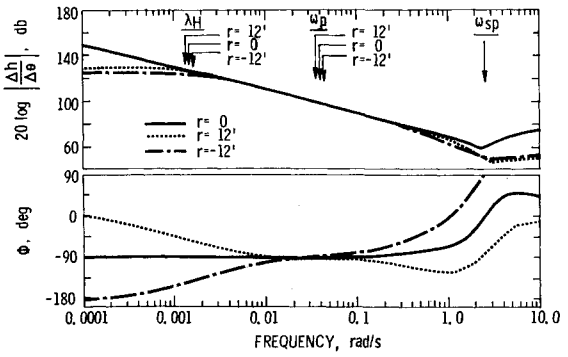

Fig. 9 Altitude/pitch angle frequency response, thrust offiset effects.

The asymptotic slope of $|\Delta h/\Delta\theta|$ shifts to +20 db/decade at the zeros, eventually dropping to zero slope upon reaching the remaining high-frequency pole (not plotted).

Thrust offset limits low-frequency response and shifts the remaining pole to much lower frequency (below the short period frequency but higher than the phugoid frequency). This effect is pursued in Fig. 9, where transfer functions for both positive and negative M_u are shown. Negative M_u changes the signs of the poles and gain of $\Delta h/\Delta\theta$. Consequently, the phase angle begins at $-180°$ and shifts through 360° before reaching its high-frequency asymptote. The two d-o-f approximation remains valid in the vicinity of the phugoid frequency.

The $\Delta h/\Delta\alpha$ amplitude ratios are plotted in Fig. 10. For zero thrust offset, the dominant slope is −40 db/decade; the amplitude ratio is much increased over $\Delta h/\Delta\theta$. For an altitude oscillation at the phugoid frequency, $\Delta\alpha$ is 40–53 db below (100–450 times smaller than) the $\Delta\theta$ oscillation. With thrust offset, $\Delta\alpha$ response at that frequency is diminished by another 40 db, and the low-frequency asymptote is the $\Delta h/\Delta\theta$ asymptote.

Control Loop Closures

The dynamic stability of the aircraft can be much improved by feedback control; numerous single-loop closures and a multiloop closure are considered here. It is assumed that the short period poles are sufficiently far from the phugoid and height mode poles that there is negligible interaction for moderate-gain loop closures.

There are at least twelve control transfer functions of possible interest, and each of these can be modified by compensation or multiloop closures. Altitude, forward velocity, pitch, and angle-of-attack perturbations can be fed to thrust, lift, or moment control. Other control transfer functions are simply integrals, derivatives, or linear combinations of the previous functions.

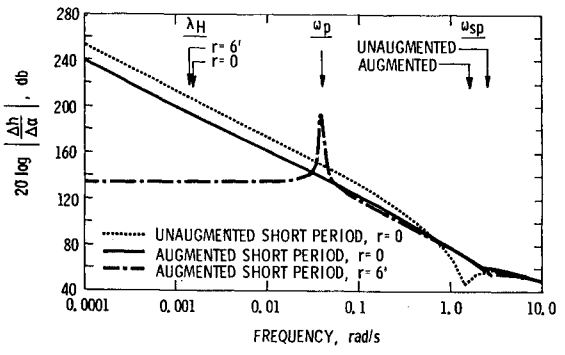

Fig. 10 Altitude/angle-of-attack frequency response.

The effects of certain control loop closures are summarized in Table 1. The observations on stability are based upon the standard case with augmented short period, no thrust offset, and no additional compensation in the control system. In Table 1, "strong" phugoid stability or instability denotes horizontal departure of the roots into the left or right half plane, while "weak" (in)stability signifies a near-vertical departure, with the roots terminating in the (right) left half plane. The "strong" criterion for the height root signifies unlimited travel along the real axis, whereas "weak" (in)-stability implies that the root's travel is blocked by a nearby zero.

Altitude feedback to thrust, lift, and moment controls is considered first. The thrust loop closure corresponds to a typical human pilot control law and will be examined in the multiloop closure. This loop closure drives the phugoid roots into the right half plane but has a strong stabilizing influence on the height mode. Lift control can be used either to stabilize the height mode or to increase phugoid frequency, depending upon feedback sign, but it always has an adverse effect on one of the roots. Strong stabilization of the height mode by moment control is prevented by the single low frequency zero, which blocks the closed loop root's travel to the left.

This blocking effect is also felt in pitch angle feedback to thrust (negative convention) and to lift and moment (positive convention). In these cases, the zero is at the origin, so the best that can be done is to force the unstable height mode to neutral stability. Strong phugoid stabilization is possible with lift control, and, to a lesser extent, with moment control (which gives strong stability by the criterion, but which limits travel of the roots).

Forward velocity feedback to thrust and moment has similar effects on the phugoid and height modes: λ_h is shifted to the left and the phugoid roots are stabilized. For-

Table 1 Some feedback effects for the standard case, with augmented short period, no thrust offset, and no compensation [feedback is negative, unless denoted by (+)]

Feedback variable & control	Height mode	Phugoid mode
Attitude to		
thrust	SS	SI
lift (−)	I	S
lift (+)	SS	I
moment (−)	S	I
moment (+)	SI	S
Pitch angle to		
thrust	N	I
lift (−)	I	SS
lift (+)	N	SI
moment (−)	I	SS[a]
moment (+)	N	SI
Forward velocity to		
thrust	SS	SS[a]
lift (−)	SI	SS
lift (+)	N	SI
moment	SS	SS[a]
Angle of attack to		
thrust	N	SS
lift (−)	SI	SI[a]
lift (+)	N	SS
moment (−)	?	I
moment (+)	?	SS[b]

S = Stability
SS = Strong stability
I = Instability
SI = Strong instability
N = Tends to neutral stability

[a] With limited travel.
[b] Conditional stability.

ward velocity feedback to moment control is considered in the multiloop closure.

Angle-of-attack feedback to thrust and lift (positive convention) neutralizes the height mode and stabilizes the phugoid strongly. The near cancellation of a zero and λ_h makes travel of that root difficult to predict with moment control, while positive feedback produces conditional phugoid stability.

Compensation or multiloop closure is required to keep altitude under control and stabilize both modes of motion. The combination examined here is the altitude/thrust and forward velocity/moment multi-loop closure. The latter is chosen as the "inner" loop, i.e., the loop to be closed first. Figure 11a shows the root loci for negative feedback. A moderate gain maximizes phugoid damping, stabilizes the height mode, and prevents short period instability (the short period roots are not shown).

The altitude/thrust zeros are near the short period poles, and the coupling numerator ($N_{\delta T}{}^{h}{}_{\delta M}{}^{u}$) is a pure gain; therefore, the "outer" loop closure plotted in Fig. 11b involves three poles whose roots approach asympotes of ± 60 and $-180°$. The phugoid is destabilized moderately, limiting outer loop gain. To obtain tighter altitude control with this closure, the inner loop would be required to provide stronger phugoid stability, as by pitch/lift, angle of attack/thrust, or angle of attack/lift (positive) loop closures. The last closure would reduce effective lift slope, which would reduce gust response as a byproduct.

Although Table 1 is compiled for the standard case, control numerators for all cases in the parameter sweep have been calculated. For most cases, zeros remained in the same relative position. For example, those near phugoid poles stayed near the poles. In several cases, relative position is reversed. The real altitude/lift zero is usually larger than λ_h, and the altitude/moment zero is smaller than λ_h. For several thrust-offset cases, the first pair reverse; in the thrust-slope sweep, the second pair reverse. Pitch and forward-velocity zeros lying at the origin, with zero thrust offset, become positive with positive thrust offset. Positive thrust offset also moves thrust and lift zeros from the origin to become complex pairs for angle-of-attack feedback.

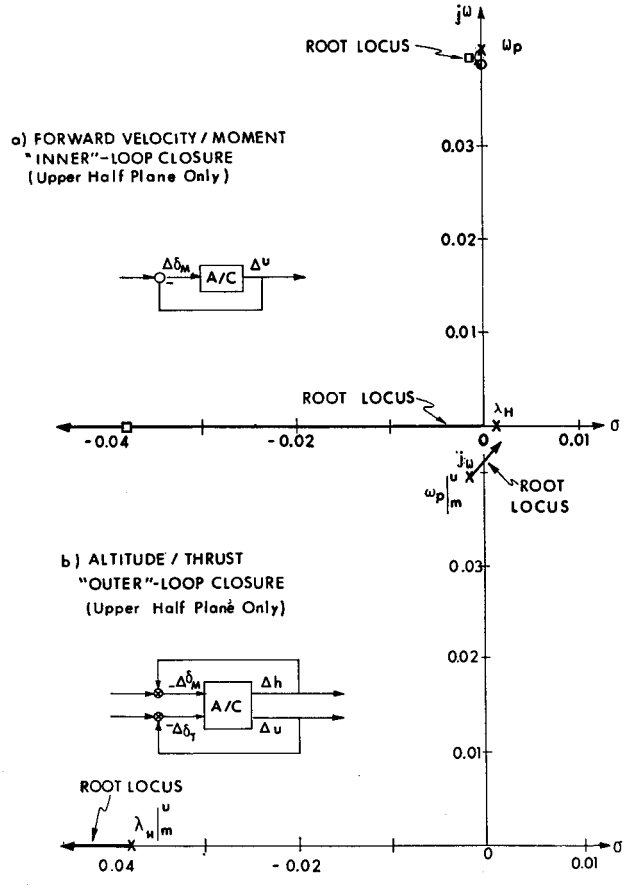

Fig. 11 Root loci with multiloop closures.

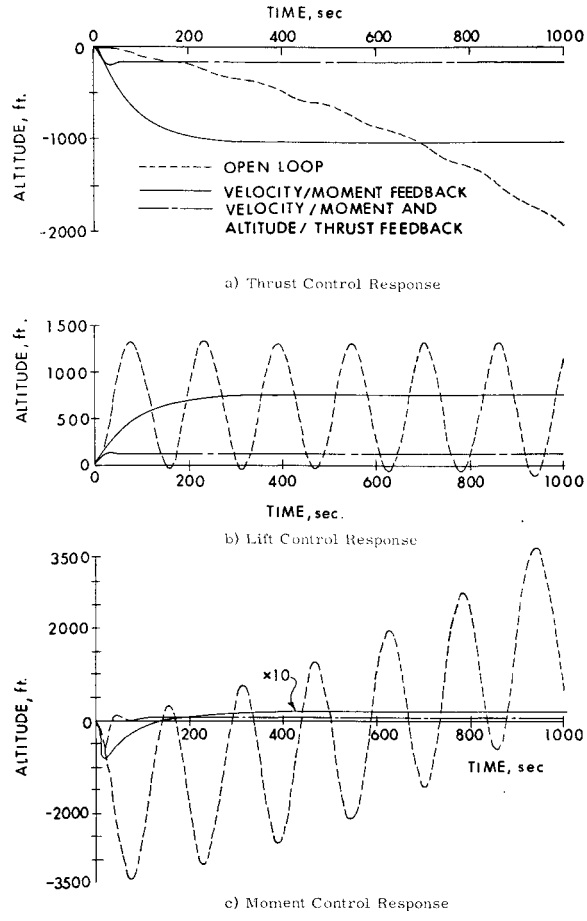

Fig. 12 Altitude response to control inputs.

Input and Disturbance Response

Time histories of the standard case's response to a number of step inputs and a turbulence profile have been computed. The 6-ft thrust offset and augmented short period stability are assumed. These time histories of altitude deviation have been obtained by numerical integration of the linear dynamical equations. Measured T_p, ζ_p, and τ_h are within 5% of the analytical values, which are 156, -0.00065, and 726 sec.

Control responses are plotted in Fig. 12. A small decrease in thrust excites the unstable height mode of the basic aircraft, causing an altitude divergence which shows only traces of the phugoid mode. During the 1000-sec descent, the pitch angle averages $-0.05°$ and does not exceed $-0.107°$, indicating the extreme sensitivity of altitude to pitch angle at three times the speed of sound. Angle of attack has reached only $-0.022°$ by the end of the period. The strongest indicator of divergence is forward velocity, which has dropped by 284 fps.

Closing the velocity/moment loop stabilizes the motion. The aircraft executes a constant-velocity dive (with minimum attitude of $-0.27°$) to a new equilibrium altitude, losing 1000 ft and one-half fps in the process. The altitude/thrust closure increases the throttle to cut altitude and velocity loss to 168 ft and 0.1 fps, incidentally decreasing phugoid stability as predicted.

Lift control of the basic airplane stimulates the phugoid with negligible effect on the height mode. The open-loop oscillation diverges slowly, with initial peak-to-peak velocity

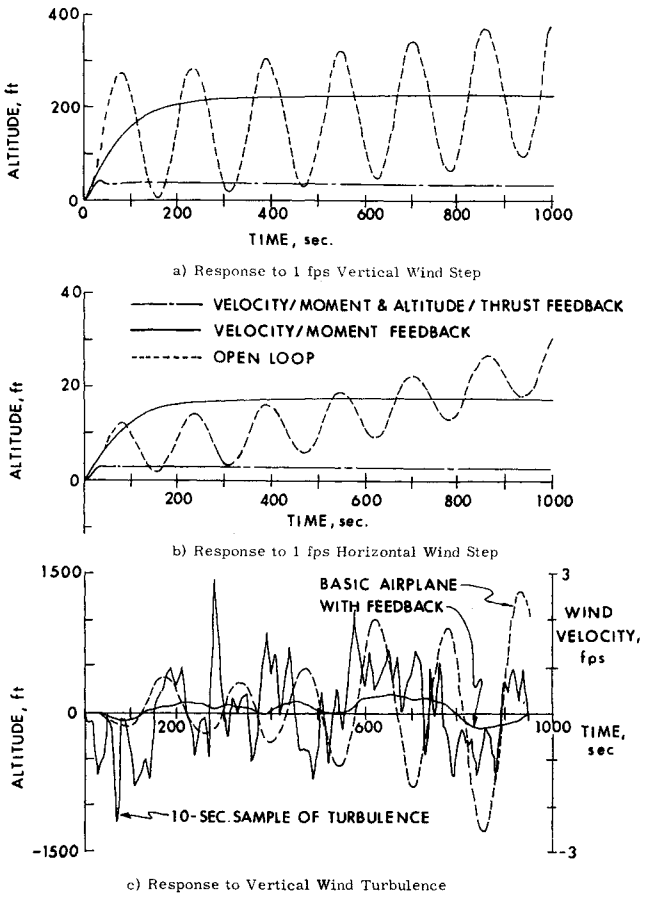

Fig. 13 Altitude response to wind inputs.

and pitch amplitudes of 30 fps and 0.1°. Controlling velocity virtually eliminates the oscillation, and altitude control reduces altitude change to 123 ft.

A pitch-down input excites both divergent modes in the basic configuration. Remarkably, the height divergence is up, the result of the 60 fps excess velocity at the bottom of the first phugoid oscillation. During the 1000 sec shown, velocity climbs to 623 fps excess, greater than the limitations imposed by the linear analysis. Initial peak-to-peak attitude oscillation is nearly 0.3°. The velocity/moment closure reduces the maximum altitude perturbation to −80 ft and the steady-state value to −17 ft, while the altitude loop further reduces these numbers to −67 and −3 ft.

Altitude response to winds is illustrated in Fig. 13. A 1-fps vertical wind initiates oscillations of 280-ft peak-to-peak amplitude and starts a steady divergence. Response with velocity feedback is overdamped and bounded, but the steady-state deflection is large. Altitude feedback reduces the steady-state response by a factor of seven. In some respects, open-loop response to a 1-fps headwind may be preferable to response with the velocity loop closure. Although oscillatory and divergent, the open-loop response is below the closed-loop response for nearly 10 min. Adding the altitude closure, the closed-loop response is decidedly superior.

The vertical wind turbulence synthesized for these tests is Gaussian Markov noise with zero mean, 1-fps standard deviation, and 100-sec period. Thus, the spectrum is relatively flat at the height and phugoid frequencies and is attenuated at the short period frequency. The turbulence is sampled at 0.1-sec intervals, although the plot in Fig. 13c is sampled at 10-sec intervals and is, therefore, heavily aliased. The basic aircraft is unstable, and its turbulence response is unbounded; however, standard deviations for the 950-sec test period can be compared with the closed-loop values. The open-loop turbulence response is merely excitation of the phugoid and does not imply any attempt to follow the wind. Altitude standard deviations for the open-loop, velocity-loop, and velocity-plus-altitude-loop cases are 527, 108, and 102 ft. The similarity of the closed-loop cases is due to the rapidly changing wind profile and the slow adjustment of the altitude loop.

If one of four engines loses thrust without "unstarting" any of the others, altitude response will look like Fig. 14.† At the termination time of the open-loop computation, over 600 fps had been lost, and altitude had decreased by 5000 ft. The altitude divergence should be well within the pilot's control capabilities. He might find the open-loop response preferable to the velocity loop response, for the constant-velocity dive results in a pitch over to nearly −2° and an altitude loss of 7300 ft. Addition of the altitude closure provides more acceptable response; however, it is unlikely that the remaining three engines can supply the 128% of cruising thrust necessary to perform the maneuver (throttle-up in response to decreasing altitude).

Atmospheric state disturbances are not plotted. Their response shapes are virtually identical to the lift control response (Fig. 12b), as induced moments are small and thrust and drag changes are assumed to cancel. Within this paper's assumptions, per centage changes in air density and pressure have identical results. In Fig. 12b, the first peak of the open-loop oscillation is 375 ft for a 1% change in density or pressure. With loop closures in the usual order, steady-state deflections are 214 and 35 ft for this change. A 1°F temperature change at 70,000-ft altitude causes an initial open-loop amplitude of 161 ft and closed-loop steady-state deviations of 92 and 15 ft.

Changes in the atmospheric state can also affect the instruments by which flight conditions are reckoned. The 1% pressure change causes a 214-ft pressure altitude change at 70,000 ft; therefore, the altitude increase would go unnoticed with the velocity closure. The barometric reference altitude for an altitude closure also would change; thus, it is likely that either system would fly an isobaric profile with 40–300-sec lag. If this is unacceptable, blending of inertial or radar altitude data is required.

Time histories for an aircraft cruising at Mach 6 and 115,000 ft are similar to the Mach 3 results. For these runs, W/S is 120 psf, L/D is 4, and ν' is +3. With augmented short period but open altitude and velocity loops, τ_h is 399 sec, while ζ_p and T_p are 0.000046 and 160.8 sec. The height divergence occurs at a faster rate, but the phugoid is barely stable. Obvious amplitude reductions are obtained from the increased W/S and decreased L/D. Response to vertical wind turbulence is reduced to a 47-ft standard deviation by the increased wing loading and the stabilized phugoid.

IV. Conclusions

The altitude stability of a supersonically cruising aircraft is dependent on the phugoid and height modes of longitudinal motion. Seemingly subtle parameters, such as air density gradient and thrust-velocity profiles, have significant effects on these long-term motions. For a range of flight conditions, these modes have been shown to be unstable, or at best, very lightly damped. The nature of altitude motion varies little with cruising altitude and Mach number, although the length scale of the phugoid and the height-mode time constant increase with Mach number. Lift/drag has a similar effect of τ_h and also affects the magnitude of phugoid stability or instability. Wing loading has little effect on the stability of either mode. Thrust law slope has a strong effect on stability, with large positive values destabilizing both the phugoid and height modes. Moments due to velocity and altitude change have a significant effect on altitude stability.

† "Jet upset" initiated by asymmetric thrust is not considered here.

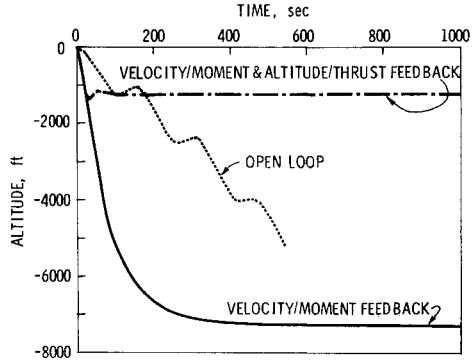

Fig. 14 Altitude response to engine unstart.

In no case should the height mode be overlooked in control system design, as many disturbances have greater effect on that mode than on the phugoid.

Short period dynamics of the aircraft have little influence on altitude stability (provided, of course, that the short period mode itself is stable), but pitch damping does act to increase phugoid damping. The combined effects of increased angle-of-attack stability and pitch damping act to decrease the phugoid period by a few seconds at most, except in cases of large $|M_u|$ and $|M_h|$, where the change may be more pronounced.

Disturbances that induce normal force or pitch moment have their greatest effect on the phugoid mode; those producing axial force have greater influence on the height mode. Thus, response to vertical wind and atmospheric state variations tends to be oscillatory, while horizontal wind and engine "unstart" produce real divergences.

By common concepts of stability, the instabilities encountered in supersonic flight are not large: negative damping ratios have small magnitude, and divergence times of the real mode measure several hundred seconds. The alert pilot should not experience difficulty in perceiving the instabilities, if he is given adequate instruments. For pitch attitude to provide a useful altitude hold cue in Mach 3 flight, a resolution of at least 0.1° is called for. Should atmospheric state disturbances of a few percent occur with any frequency, air-relative instruments will be insufficient for tight altitude control. Instrument requirements are far more severe than for subsonic flight.

Published accounts of flight tests in supersonic and variable stability aircraft suggest, however, that the greater issue of operating a supersonic aircraft within an air traffic control system is not whether a pilot can successfully close the altitude control loop, but if he can do so for hours on end with an unstable system that is continually excited by small atmospheric disturbances. Relatively simple, multiloop control closures can stabilize the system for manual control or altitude hold.

References

[1] Plattner, C. M., "Military Tests May Preview SST Problems," *Aviation Week & Space Technology*, Vol. 87, No. 16, 1967, pp. 61–62.

[2] McLaughlin, M. D. and Whitten, J. B., "Pilot Evaluation of Dynamic Stability Characteristics of a Supersonic Transport in Cruising Flight Using a Fixed-Base Simulator," TN D-2436, 1964, NASA.

[3] McLaughlin, M. D., "Simulator Investigation of Maneuver Speed Increases of an SST Configuration in Relation to Speed Margins," TN D-4085, 1967, NASA.

[4] Carriou, A. et al., *The SST*, British Air Line Pilots Association Technical Symposium, Nov. 28–30, 1967.

[5] Newell, F. and Campbell, G., "Flight Evaluations of Variable Short Period and Phugoid Characteristics in a B-26," TR 54-594, 1954, Wright Air Development Center, Wright-Patterson Air Force Base, Ohio.

[6] Lanchester, F. W., *Aerodynamics*, Arnold Constable, London, 1907.

[7] Scheubel, F. N., "The Effect of Density Gradient on the Longitudinal Motion of an Aircraft," *Luftfahrtforschung*, Vol. 19, No. 4, 1942, pp. 132–136; R. T. P. Translation 1739.

[8] Neumark, S., "Longitudinal Stability, Speed and Height," *Aircraft Engineering*, Vol. 22, Nov. 1950, London, pp. 323–334.

[9] Etkin, B., "Longitudinal Dynamics of a Lifting Vehicle in a Circular Orbit," UTIA Report 65, 1960, Univ. of Toronto; also TN 60-191, 1960, Air Force Office of Scientific Research.

[10] Larrabee, E. E., "Aerodynamic Penetration and Radius as Unifying Concepts in Flight Mechanics," *Journal of Aircraft*, Vol. 4, No. 1, Jan.-Feb. 1967, pp. 28–35.

[11] Seckel, E., *Stability and Control of Airplanes and Helicopters*, Academic Press, New York, 1964.

[12] McRuer, D. T., Ashkenas, I. L., and Pass, H. R., "Analysis of Multiloop Vehicular Control Systems," ASD-TDR-62-1014, March, 1964, Wright-Patterson Air Force Base, Ohio.

[13] *U. S. Standard Atmosphere, 1962*, NASA, Washington, D. C. 1962.

[14] Nielsen, J. N., *Missile Aerodynamics*, McGraw-Hill, New York, 1960.